In-situ measurements of release characteristics and catalytic effects of different chemical forms of sodium during combustion of Zhundong coal

Yingzu Liu[1,3], Zhihua Wang[1], Kaidi Wan[1,*], Yu Lv[2,*], Jun Xia[3], Yong He[1], Kefa Cen[1]

1. State Key Laboratory of Clean Energy Utilization,
Zhejiang University, Hangzhou 310027, China

2. Department of Aerospace Engineering, Mississippi State University,
Mississippi State, MS 39762, USA

3. Department of Mechanical and Aerospace Engineering & Institute of Energy Futures,
Brunel University London, Uxbridge UB8 3PH, UK

* Corresponding authors: wankaidi@zju.edu.cn (Kaidi Wan); ylv@ae.msstate.edu (Yu Lv).

Abstract

This work studies the temporal release characteristics of different chemical forms of sodium during the combustion of Zhundong coal and the catalytic effects of sodium on the combustion process via target-sodium removal and enrichment approaches. The target-sodium removal approach extracts specific forms of sodium from the raw coal via a chemical method to produce coal samples with designated characteristics. In the target-sodium enrichment approach, three kinds of H_2O-soluble sodium compounds, including NaCl, NaOH and Na_2SO_4, are manually added into the raw coal. The experimental measurement is conducted using a multi-point Laser-Induced Breakdown Spectroscopy (LIBS) system. The system quantitatively measures the temporal release flux of sodium during the combustion process, and performs the in-situ measurement of surface temperature and diameter of a burning coal pellet. It is found that H_2O-soluble sodium is the major chemical form of sodium released during the combustion and exhibits the highest volatility. All the three forms of enriched H_2O-soluble sodium compounds show a catalytic effect on the coal combustion (burnout

time decreased by more than 5.7%) and the catalytic activity of NaOH is found to be the strongest (burnout time decreased by 36.8%).

Keywords: Zhundong coal; Sodium; Alkali metal; Catalytic effects; Laser-Induced Breakdown Spectroscopy

1. Introduction

Coal, as an important source of primary energy, supports approximately 40% of the worldwide electricity [1, 2]. Considering its broad availability and the overall flexibility of coal combustion systems, coal is expected to continually play an important role in the near future [3, 4]. In practice, the presence of alkali metals, especially sodium (Na), in coals leads to severe ash-related issues, such as fouling, slagging and corrosion [5]. The sodium released from the combustion process can condense on the heat transfer surfaces and form an initial sticky layer, which leads to rapid ash deposition [6, 7]. Furthermore, through reacting with sulfur and chloride species, sodium can also form complex sulfur and chloride compounds, which causes fouling and corrosion damages [8]. These sodium-induced issues severely limit the utilization of coals that have a relatively high concentration of sodium, such as the Zhundong coal which can potentially serve as the main energy source for China for the next 100 years [9-11]. To enable clean utilization of the Zhundong coal requires better understanding on the sodium-release characteristics during the coal combustion process [12].

The detailed studies on the sodium release characteristics during coal combustion rely on advanced measurement techniques. Over the past decade the measurement techniques in this regard have evolved from offline measuring techniques to online in-situ measurements using laser

diagnostics. Offline sampling measurements typically employ chemical analysis methods, such as the inductively coupled plasma atomic emission spectroscopy (ICP-AES), to obtain the composition and mass of sodium species present in the fly ash or ash deposits in the post-combustion stage [13]; while online techniques, e.g., Laser-Induced Fragmentation Fluorescence (ELIF) [14], Tunable Diode Laser Absorption Spectroscopy (TDLAS) [15], Planar Laser-Induced Fluorescence (PLIF) [16] and Laser-Induced Breakdown Spectroscopy (LIBS) [17], can directly and accurately capture the time-resolved sodium release process during the combustion. In our recent studies, the release characteristics of atomic sodium and sodium element during the combustion of Zhundong coal pellets are quantitatively measured using PLIF [18] and multi-point LIBS methods [19].

The previous studies [20, 21] identified that the sodium in coal can be classified into four chemical forms: (1) H_2O-soluble sodium, which exists as sodium salts; (2) CH_3COONH_4 (NH_4Ac)-soluble sodium, which is bounded to carboxyl groups; (3) HCl-soluble sodium, which is organically bounded to oxygen- or nitrogen-containing functional groups; (4) insoluble sodium, which is attached to minerals. The sum of NH_4Ac-soluble and HCl-soluble sodium is also called organically-bound sodium. The release characteristics of individual chemical forms of sodium have been studied using offline ICP-AES measurements [22, 23]. For instance, Liu et al. [22] investigated the transformation behavior of sodium in four high-alkali coals during the combustion process, and found that the released sodium mainly results from the NH_4Ac-soluble and H_2O-soluble sodium. Li et at. [23] showed that the H_2O-soluble and NH_4Ac-soluble sodium mainly contributes to release of total sodium during the pyrolysis process, while H_2O-soluble and insoluble sodium is primarily released during the char gasification. In the regard to online in-situ measurement, van Eyk et al. [24] measured the temporal release of water- and organically-bound sodium during the char burnout stage

of a Loy Yang coal pellet using PLIF. However, their measurement did not obtain the release profiles during the first devolatilization stage, or distinguish NH_4Ac-soluble and HCl-soluble sodium from the total organically-bound sodium.

Although alkali metal can cause severe ash-related issues, it is also found that alkali metal can have positive effects on the thermochemical conversion of solid fuels [25]. The activity of char can be enhanced in the presence of alkali metal. Kuang et al. [26] found that sodium compounds can weaken the bond of (C-O) in coal black liquor slurry, which improves the gasification conversion rate. A number of studies [27-31] have attempted to introduce extra alkali metal additives to promote the thermochemical conversion of solid fuels, such as coal and biomass. For example, Tang et al. [29] investigated the catalytic activity of three alkali carbonates (Li_2CO_3, Na_2CO_3, and K_2CO_3) towards the steam gasification of coal char, and they found that Na_2CO_3 is the most resistant to catalytic deactivation. Liu et al. [31] showed that the addition of potassium could improve the productions of H_2, CO and CO_2, while reducing the production of CH_4 during rice husk high-temperature pyrolysis. These previous studies motivate us to examine the catalytic effects of different chemical forms of alkali metal on the combustion of Zhundong coal.

In summary, the abovementioned previous studies have not revealed quantitative information on the time-resolved release characteristics of different chemical forms of sodium during coal combustion. Furthermore, the efforts on isolating and analyzing the catalytic effects of these different forms of sodium on the combustion process have not been carried out. Within this context, the objective of the present study is to investigate the time-resolved release characteristics of different chemical forms of sodium during the combustion of coal and the catalytic effects of these forms of sodium on the combustion process. To isolate the effects of the sodium of different forms, the coal

samples will be pre-processed using the target-sodium removal and enrichment treatments, and this procedure will be detailed in Section 2. The measurement will be conducted using a combination of two in-situ measurement techniques, including multi-points LIBS and two-color pyrometry. Online multi-point LIBS technique, upgraded from the single-point LIBS previously developed in [32], will be adopted to capture the time-resolved sodium release flux during the combustion of a coal pellet. A two-color pyrometer will be employed to obtain the surface temperature and diameter of the burning coal pellet. Based on these experiments, the release characteristics of different chemical forms of sodium and their catalytic effects on coal combustion can be accurately captured.

2. Experimental methodology

2.1. Coal samples

The Zhundong coal used here is the same as in our previous studies [19], which has appreciable sodium content. The proximate and ultimate analyses, as well as the ash composition of the raw coal sample are summarized in Table 1. The proximate analyses were conducted according to the Chinese National Standard GB/T 212-2008. The ultimate analyses were performed according to the Chinese National Standard GB/T 476-2008 (for C, H), GB/T 19227-2008 (for N) and GB/T 214-2007 (for S). The mass fraction of oxygen (O) was obtained by 100%-C%-H%-N%-S%. Ash compositions were identified according to the Chinese National Standard GB/T 1574-2007.

Table 1. Chemical analysis of Zhundong coal.

Proximate analysis (wt%, air dry basis)						
Moisture	Ash	Volatile	Fix Carbon			
9.85	4.23	28.72	57.2			
Ultimate analysis (wt%, dry ash free basis)						
Carbon	Hydrogen	Nitrogen	Sulfur	Oxygen		
79.29	2.89	0.88	0.43	16.5		
Ash composition (wt%)						
SiO_2	Al_2O_3	Fe_2O_3	CaO	MgO	K_2O	Na_2O
10.80	9.62	3.95	36.82	9.20	0.40	10.87

The air-dried raw coal is grounded and sieved to fine powders with the diameter of pulverized-coal particles less than 75 μm. The obtained pulverized-coal samples are used for measurement.

2.2. Target-sodium removal via chemical extraction method

The sodium removal treatment is performed via a chemical extraction method based on the solubility of different chemical forms of sodium in different solvents. 1 g of the coal sample was first added into 100 ml water at 333 K and thoroughly stirred. The mixture is then filtered, and H_2O-soluble sodium is removed in the solid residual sample. ICP-AES is employed to analyze the filtrate to determine the content of first class H_2O-soluble sodium like sodium sulfates and chlorides. The solid filter residue is then sequentially treated by 100 ml NH_4Ac (1 mol/L) and 100 ml HCl (1 mol/L), with the filtrate of each step analyzed via ICP-AES. The analysis is able to identify the

second class NH_4Ac-soluble sodium, and the third class HCl-soluble sodium. The final residual after HCl extraction is dissolved in strong acid and then analyzed using ICP-AES to obtain the information of the insoluble sodium, such as sodium silicate.

The solid filter residuals obtained in each step, with H_2O-soluble, NH_4Ac-soluble and HCl-soluble sequentially removed, are completely dried in an oven at 333 K and exposed in the air for 24 hours before further use.

2.3. Target-sodium enrichment approach

First, 1g of the coal sample and 5 mg of a sodium additive are blended in 50 ml water at 333 K. Three sodium additives, i.e., NaCl, NaOH and Na_2SO_4, which represent the most common H_2O-soluble sodium in coal [12], are added in the mixture solution. Then the mixture is continuously stirred at 333 K until the water is completely vaporized. The sodium enriched coal powders obtained through this treatment are then grounded into small sizes for further use.

The raw and target-sodium removed/enriched coal samples are employed in the LIBS measurements. 50 mg of the coal powder is pressed into a 4 mm spherical pellet. The mass of the removed/enriched sodium is negligible compared to the total mass of coal sample (< 0.5%), and the apparent densities of the coal pellet are 1492 kg/m^3.

2.4. Experimental setup

The experimental setup consists of a combustion system and a multi-point LIBS measurement system. The combustion system is shown in Fig. 1a. A spherical coal pellet is suspended on two ceramic rods (diameter of 1 mm) at a height of 10 mm above a heat flux burner. The burner is

operated with the flow rates of methane and air at 0.59 SL/min and 7.06 SL/min, respectively, to generate a laminar lean premixed methane-air flame (equivalence ratio of 0.8). The gas composition is (by volume): 3.9% O_2, 7.6% CO_2, 15.4% H_2O and 72.8% N_2, and the temperature at the pellet location is around 1892 K, based on CHEMKIN calculation using the GRI-3.0 mechanism [33].

The multi-point LIBS measurement system [19] is illustrated in Fig. 1b. An Nd:YAG laser (Spectra Physics, Model PRO-250) with a fundamental wavelength of 1064 nm is focused at the measurement point which is 10 mm above the burning coal pellet. The repetition rate, pulse duration and average laser energy are 10 Hz, 10 ns and 300 mJ, respectively. The LIBS signal is collected by a spectrometer (Ocean Optics, Model USB 4000). The spectrometer is synchronized with the laser via a digital pulse generator (Stanford Research System, DG535). In order to perform multi-point LIBS measurement, the laser focusing lens and LIBS signal collection optics are installed on an electric translational platform. The LIBS measuring point is moving periodically in the radius distance (r) of -12 mm, -9 mm, -6 mm, -3 mm, 0 mm, 3 mm, 6 mm, 9 mm, 12mm. The moving frequency of the platform is 10 Hz, which is synchronized with the laser and spectrometer, and therefore the LIBS measuring frequency at the same measuring point is 1 Hz.

To achieve the quantitative measurement of sodium concentration, the LIBS system has been calibrated by measuring the intensity of the sodium doublet (588.995 nm and 589.592 nm) in a sodium chloride (NaCl) seeded flame. The calibration procedure has been detailed in our previous study [34]. The obtained linear relationship between LIBS signal and sodium concentration is:

$$I_{LIBS,Na} = 2430 \times C_{Na},\ R^2 = 0.96, \quad (1)$$

where $I_{LIBS,Na}$ is the LIBS signal and C_{Na} is the sodium concentration (mg/m^3) at the measuring point.

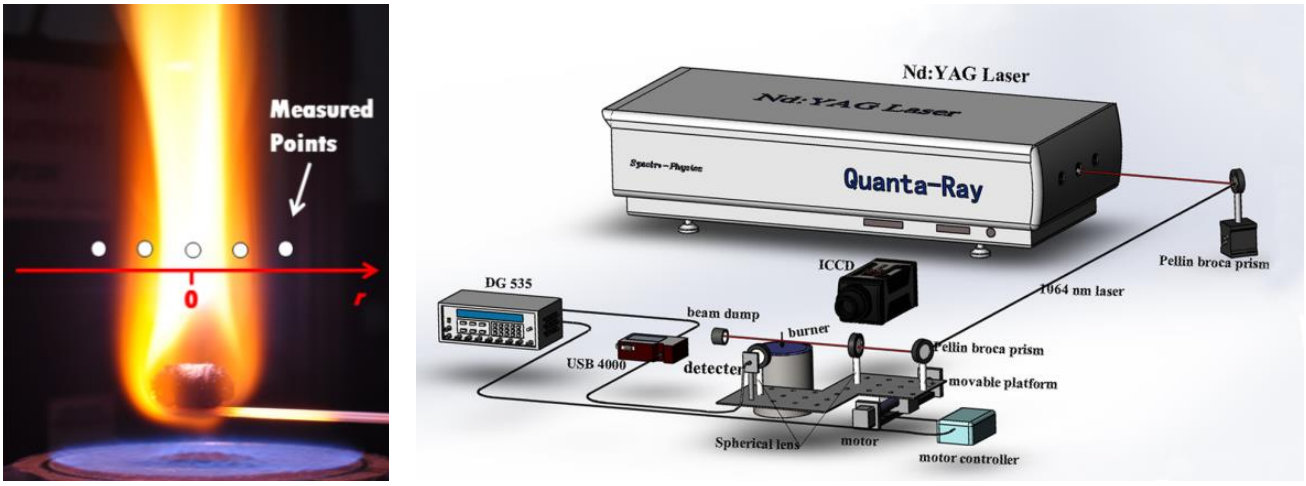

(a) LIBS measuring points (b) Configeration of equipments

Fig. 1. Multi-point LIBS experimental setup.

From the sodium concentration of all the nine measuring points, the sodium flux ($Na_{flux,t}$) passing through the measuring plane 10 mm above the burning coal pellet can be determined as:

$$Na_{flux,t} = \int_0^{2\pi} \int_0^{\infty} u \times C_{Na} \times r \times dr \times d\theta, \tag{2}$$

where u is the axial velocity and θ is the radian. In the present work, the pellet is spherical and the burner produces a uniform gas flow. Therefore, Equation (2) can be simplified as:

$$Na_{flux,t} = 2\pi \times \int_0^{\infty} u \times C_{Na} \times r \times dr\,. \tag{3}$$

Considering that the distributions of u and C_{Na} are both functions of r, the $Na_{flux,t}$ at a given time can be evaluated as:

$$u = f_u(r), \tag{4}$$

$$C_{Na} = f_{Na,t}(r), \tag{5}$$

$$Na_{flux,t} = 2\pi \times \int_0^{\infty} f_t(r) \times dr\,. \tag{6}$$

The sodium flux $Na_{flux,t}$ at different time can be determined from an integration of a function of r. In addition, integrating the sodium flux with time can provide the total amount of sodium released during the combustion of a coal pellet.

$$Na_{volatile} = \int_0^{\infty} Na_{flux,t} \times dt \,. \tag{7}$$

More details about the integrating procedures can be found in [19].

In LIBS measurement, the uncertainties come from calibration uncertainty and electronic noise. The calibration uncertainty originates from self-absorption and a higher sodium flux level can result in a higher uncertainty. In the present study, the maximum magnitude of the LIBS-calibration uncertainties of the LIBS system is 3.5E-5 mg/s (relative magnitude of 7.8%), which is found at the sodium flux of 4E-4 mg/s. The total uncertainty of the LIBS measurement is defined as the square root of the quadratic sum of the maximum calibration error and the standard deviation of three measurements.

The surface temperature of a burning coal pellet is measured using a two-color pyrometer [19]. The output of the two-color pyrometer, $I_{(\lambda,T)}$, is proportional to the radiant exitance of the measured pellet surface [35]:

$$I_{(\lambda,T)} = R_c \times S_\lambda \times \varepsilon_\lambda \times \frac{C_1}{\lambda^5} \times e^{-C_2/(\lambda T)}, \tag{8}$$

where R_c is the instrument constant [36], S_λ is the spectral sensitivity of the charge coupled device (CCD) system, ε_λ is the monochromatic emissivity. T is the temperature of pellet surface, C_1 and C_2 are the first and second Planck's constants. By using Wien's equation to compare $I_{(\lambda,T)}$ at two different wavelengths, the surface temperature is determined as [35]:

$$T = \frac{C_2\left(\frac{1}{\lambda_2} - \frac{1}{\lambda_1}\right)}{\ln\frac{I_{\lambda_1}}{I_{\lambda_2}} + \ln\frac{S_{\lambda_1}}{S_{\lambda_2}} + \ln\frac{\varepsilon_{\lambda_1}}{\varepsilon_{\lambda_2}} + \ln\frac{\lambda_1^5}{\lambda_2^5}} \,. \tag{9}$$

To correct the spectral response of both the CCD and filters, the value of $S_{\lambda 1}/S_{\lambda 2}$ is calibrated by measuring a thermocouple in the flame. The temperature obtained by the thermocouple is served as the standard for the calibration.

In the present study, a bi-optic lens attachment (Model: LAVISION VZ-image doubler) is used to record two-dimensional (2D) images of a coal pellet at 1 Hz. Two filters with a bandwidth of 1 nm, which centered at 633 nm and 647 nm, provide the spectral discrimination required for the two-color pyrometry. Because the two wavelengths are close to each other, $\varepsilon_{\lambda 1}/\varepsilon_{\lambda 2}$ is approximated by 1.

During the combustion of a coal pellet, its shape can be identified from the 2D images of thermal irradiation [37]. The diameter of the pellet is then determined from the average between two orthogonal dimensions in the images under the two wavelength. The uncertainty of the two-color measurement is calculated as the standard deviation of three measurements.

3. Results and discussions

3.1. Release characteristics of different chemical forms of sodium

The contents of the different chemical forms of sodium in the Zhundong raw coal are summarized in Table 2. The mass of Na (mg) in a sample prepared from 1 g of the Zhundong raw coal is determined by performing the ICP-AES measurements on the filtrate of chemical extraction method, as described in Section 2.2. It can be found that the major chemical forms of sodium in the Zhundong raw coal are H_2O-soluble (34.3%) and insoluble (46.8%) sodium, while the concentrations of the other two chemical forms, i.e., NH_4Ac-soluble and HCl-soluble sodium, are very marginal.

229 Table 2. The content of different chemical forms of sodium in Zhundong raw coal measured by

230 ICP-AES.

	Na content in a coal pellet (50 mg)				
	H_2O-soluble	NH_4Ac-soluble	HCl-soluble	Insoluble	Total
Mass (mg)	0.13±0.006	0.05±0.003	0.02±0.003	0.17±0.007	0.37
Percentage	34.3%	12.6%	6.1%	46.8%	100.0%

231

232 Temporal release of different chemical forms of sodium during combustion is shown in Fig. 2.
233 Time resolution of the profiles is 1 data point per second. By employing the division method
234 described in [19], three characteristic stages of coal pellet combustion can be determined for the raw
235 and H_2O treated coal samples: (1) a narrow peak during the devolatilization stage; (2) a left skewed
236 large peak during the char burnout stage; (3) a gradual decrease during the ash cooking stage. For the
237 NH_4Ac treated sample, the three stages can also be identified in its sodium flux profile but the
238 magnitude of the peaks are much smaller. In contrast, the profile of the HCl treated sample does not
239 show the three-stage characteristics: only one gentle peak is found at the devolatilization stage and
240 the sodium flux is smaller compared to other cases.

241

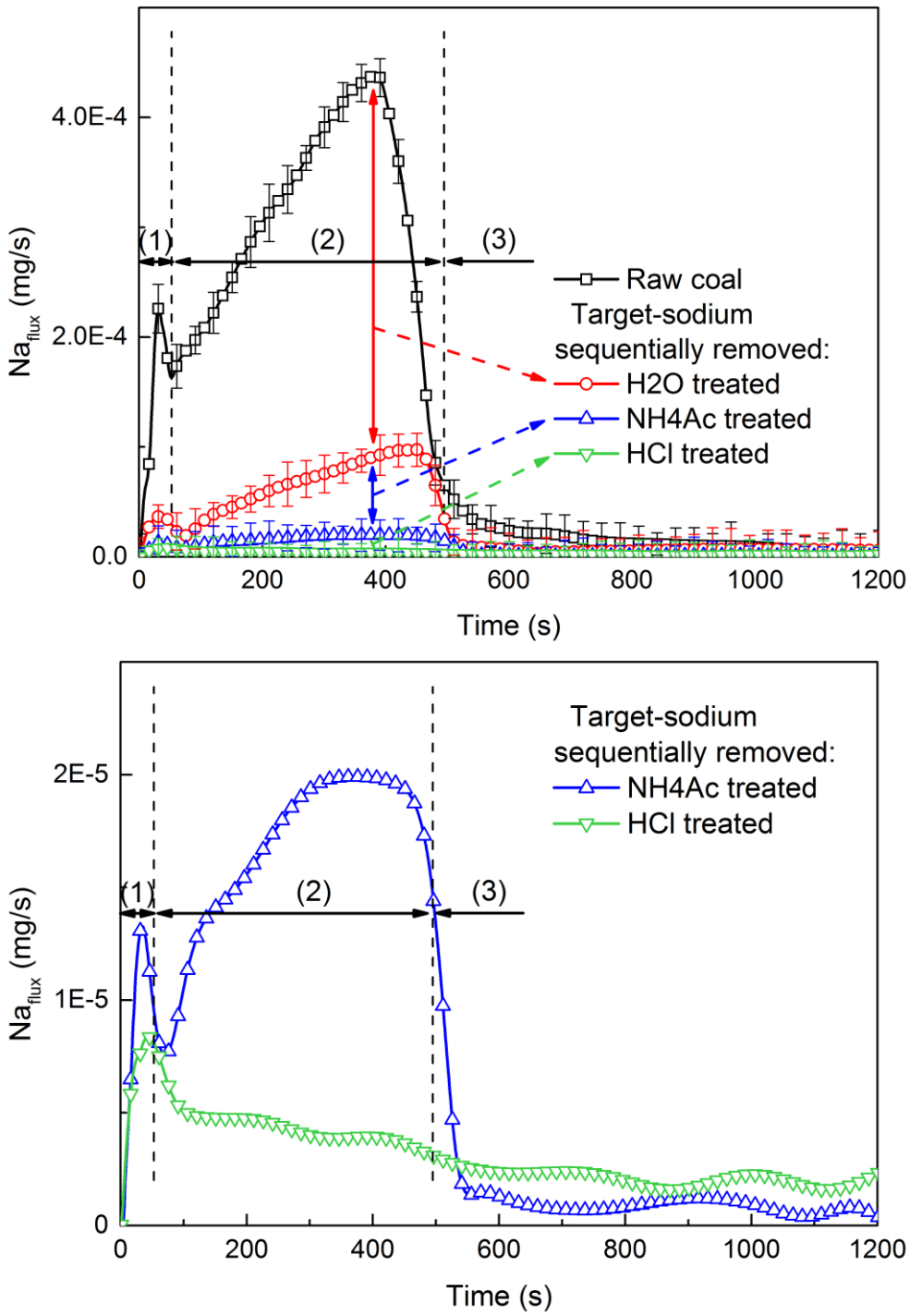

Fig. 2. Temporal sodium release profiles of raw and target-sodium sequentially removed Zhundong coal measured by the multi-point LIBS. Three combustion stages for the raw coal pellet are illustrated: (1) devolatilization, (2) char burnout, and (3) ash cooking. The NH_4Ac and HCl treated cases have been zoomed in and shown on the bottom.

By integrating the sodium flux with the time, the mass of sodium released at the three stages of coal pellet combustion for the four samples can be identified, as listed in Table 3. Comparing the sodium released at the three stages for raw Zhundong coal, it can be observed that the char burnout stage contributes to 86.7% of the total sodium release, while the devolatilization and ash cooking stages only release a minor amount, i.e., 5.1% and 7.3%, respectively. The durations of the three combustion stages for the four samples are also summarized in Table 3. Since the termination time of devolatilization stage for the HCl treated sample is difficult to identify, the same value as NH_4Ac treated sample is used. It can be found that the removal of sodium results in a longer devolatilization and coal burnout time. This can be attributed to the catalytic effects of sodium on the combustion, which will be further elaborated in Section 3.3.

Table 3. Sodium released at the three stages of the combustion of raw and target-sodium sequentially removed Zhundong coal. Time periods of the three stages are summarized in parentheses.

Sample	Na released (mg/coal pellet)			
	Devolatilization	Char burnout	Ash cooking	Total
Raw coal	7.6E-3 (0-53 s)	1.3E-1 (53-495 s)	1.1E-2 (495-1200 s)	1.5E-1
Target-sodium sequentially removed				
H_2O-soluble	2.0E-3 (0-73 s)	2.9E-2 (73-507 s)	4.7E-3 (507-1200 s)	3.6E-2
NH_4Ac-soluble	6.0E-4 (0-70 s)	7.5E-3 (70-540 s)	5.9E-4 (540-1200 s)	8.7E-3
HCl-soluble	4.6E-4 (0-70 s)	-	-	3.9E-3

Based on the difference between the sodium release from the four samples, the contribution of

265 different chemical forms of sodium to the mass of sodium released in the three stages of coal pellet
266 combustion can be evaluated, as shown in Fig. 3. Since the char burnout and ash cooking stages for
267 the HCl treated sample (insoluble sodium remains) cannot be identified, the sum of the HCl-soluble
268 and insoluble sodium is shown for these two stages. It is noted that the H_2O-soluble sodium is the
269 major chemical form of sodium released in every stage, contributing to 76% of the total sodium
270 released during the entire period of coal pellet combustion. The contributions of different chemical
271 forms of sodium are similar for each stage: The H_2O-soluble sodium plays the dominant role; the
272 NH_4Ac-soluble sodium is the second largest contribution; and the contributions of the HCl-soluble
273 and insoluble are marginal. Comparing the mass of sodium released (Table 4) detected by
274 multi-point LIBS measurement to the sodium content in the raw Zhundong coal (Table 2) identified
275 via ICP-AES, the ratio of the released sodium mass to the existing sodium mass can be deduced for
276 different forms of sodium. It can be found in Table 4 that 40.7% of the sodium contained in the raw
277 coal is released into the gas phase during the whole period of coal pellet combustion. The release
278 ratio reflects the volatility of different chemical forms of sodium. The H_2O-soluble sodium shows the
279 highest volatility with a release ratio of 90.1%, while the insoluble sodium is in a much more stable
280 chemical state because only 2.3% of its mass is released during the combustion.
281

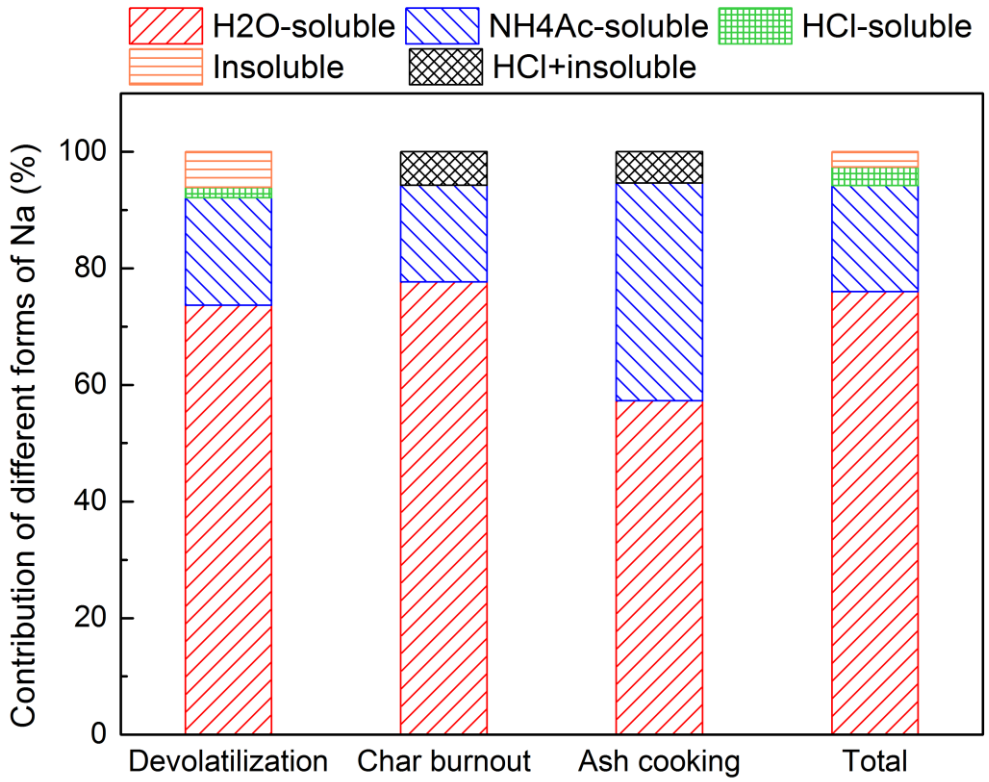

Fig. 3. Contribution of different chemical forms of sodium to the mass of sodium released in the three stages of coal pellet combustion.

Table 4. Released mass and release ratio of the sodium contained in the raw coal for different chemical forms of sodium during coal pellet combustion measured by multi-point LIBS.

Chemical forms	Released mass (mg)	Release ratio (%)
H_2O-soluble	0.114	90.1
NH_4Ac-soluble	0.027	58.7
HCl-soluble	0.005	21.3
Insoluble	0.004	2.3
Total	0.150	40.7

3.2. Release characteristics of different H_2O-soluble sodium

As the H_2O-soluble sodium is found to be the dominant chemical form of sodium released during the entire period of combustion, the release characteristics of different forms of H_2O-soluble sodium are then investigated by measuring the sodium enriched coal pellets. The temporal sodium concentration profiles of the raw and target-sodium enriched coal are presented in Fig. 4a. The sodium release is found to be much stronger for the sodium enriched samples than the original raw coal, because the content of sodium, especially the highly-volatile H_2O-soluble sodium, is much higher in the sodium enriched samples (Table 5) than in the raw coal (Table 2). The second sodium release peak corresponding to the char burnout stage occurs earlier for sodium enriched samples, which is due to the following reasons: (1) The enriched sodium catalyzes char combustion by forming -CNa and -CONa, which leads to a shorter burning period and more intensive combustion process. Thus, the release of raw sodium in the sample is enhanced [38]. (2) The enriched sodium can directly evaporate into the gas phase in the high temperature combustion environment. Table 6 summarizes the time at termination of the char burnout stage for the four samples including the raw and sodium enriched coal pellets. After the coal pellet is enriched with NaOH which has the highest catalytic effects, the burnout of the pellet is shortened by 36.8%.

By subtracting the profiles of target-sodium enriched and raw coal pellets and normalizing the time with the characteristic time of char burnout in each case, the temporal sodium release characteristics of the three enriched sodium can be better estimated, and the post-processed results are shown in Fig. 4b. Profiles of the raw coal and originally contained H_2O-soluble sodium are also shown as a reference. The concentration of released Na_2SO_4 is much lower than the other two forms of sodium, which suggests that the volatility of Na_2SO_4 during coal combustion is weaker. The

311 release characteristics of the enriched H_2O-soluble sodium are found to be different from the original
312 one, which implies a complex release mechanism of the original sodium. The H_2O-soluble sodium is
313 not only released through the volatilization process under high temperature, but also gradually
314 released along with the collapse of micro-pores during the heterogeneous combustion of coal. Thus,
315 the release of original sodium is delayed.

316

317 Table 5. Mass of sodium contained in different target-sodium enriched Zhundong coal pellets.

Samples	Na content (mg) in a coal pellet (50 mg)		
	Enriched mass of Na	Total H_2O-soluble Na	Total
0.5% NaCl enriched	0.10	0.23	0.47
0.5% Na_2SO_4 enriched	0.08	0.21	0.45
0.5% NaOH enriched	0.14	0.27	0.51

318

319

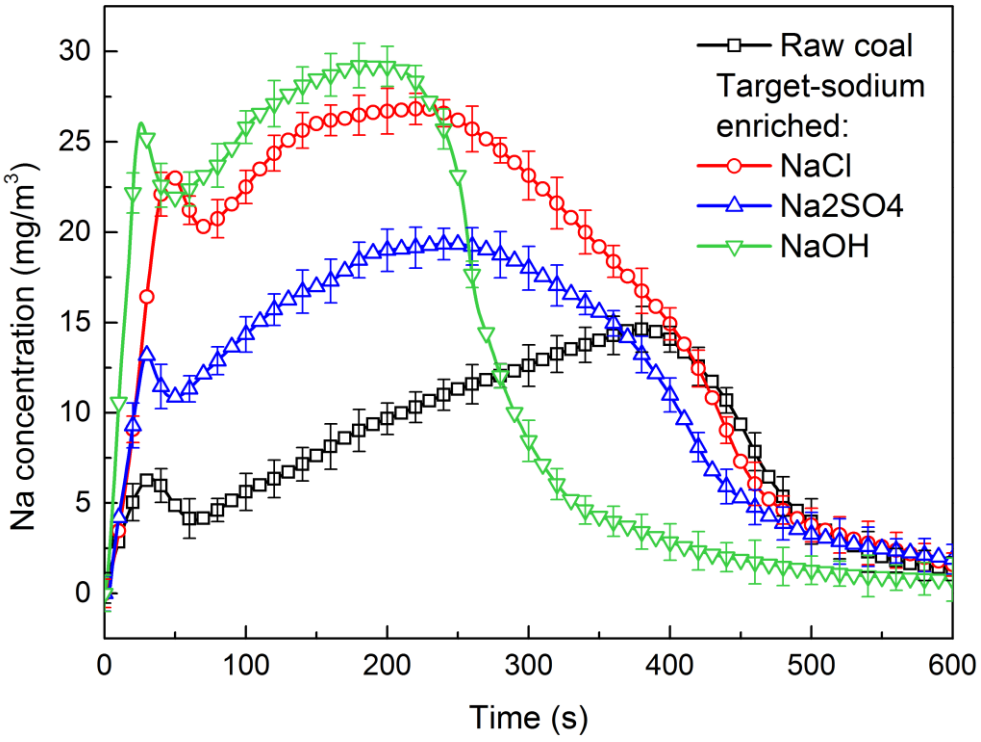

(a) Temporal sodium release profiles

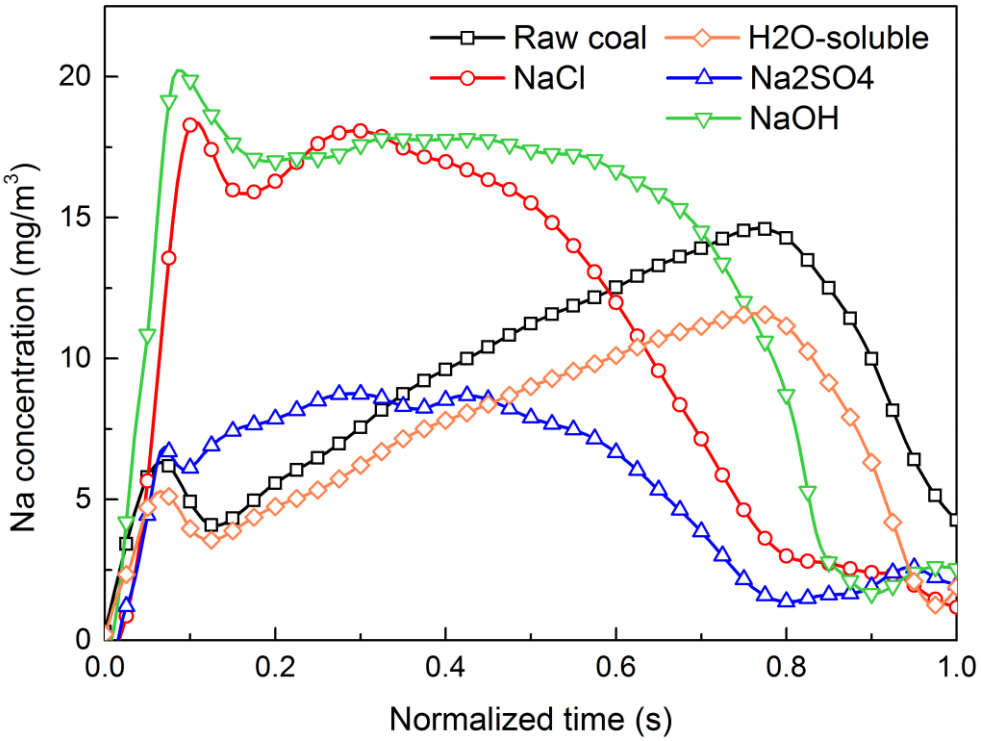

(b) Time-normalized sodium release profiles

Fig. 4. (a) Temporal sodium release profiles of raw and target-sodium enriched Zhundong coal measured by single-point LIBS. (b) Time-normalized temporal release profiles. The time has been normalized by the characteristic time at the termination of char burnout in each case. Profiles of the

raw coal and originally contained H_2O-soluble sodium are also shown.

Table 6. Time at termination of the char burnout stage for raw and target-sodium enriched Zhundong coal.

Samples	Time at termination of char burnout (s)
Raw coal	495
NaCl-enriched	467
Na_2SO_4-enriched	436
NaOH-enriched	313

3.3. Catalytic effects of the sodium on coal pellet combustion

The catalytic effects of different chemical forms of sodium on coal pellet combustion are examined. Figure 5 shows the temporal profiles of surface temperature and diameter of four different coal pellet samples for raw and target-sodium sequentially removed Zhundong coal, which are recorded in real-time during the combustion. The general trends of the profiles for the four samples are similar. In the beginning, the coal pellet is rapidly heated up in the hot environment. Then the pellet starts to devolatilize and volatiles burn around the pellet. Heated by the burner-produced methane-air flame and the volatile flame, the surface temperature of the coal pellet increases to about 1700 K within a few seconds. After the volatiles burn out, the pellet temperature reaches an inflection point since the heating effect from the volatile flame disappears. Because the duration of the first devolatilization stage is relatively short, the diameter of the coal pellet does not change significantly. In the second char burnout stage, the heterogeneous combustion between solid char and

gas-phase surroundings takes place, which generates new heat source and shrink the coal pellet. When the pellet is close to burnout, its temperature decreases because char combustion is weak and therefore the heat loss to the surroundings becomes larger than the heat produced from the combustion. After char burnout, the residual ash reaches a stable chemical state in the third ash cooking stage. The pellet temperature and diameter at this stage are almost constant, and therefore not shown for brevity.

For the cases with target-sodium removal treatment, the characteristic profiles of pellet temperature and diameter are found to be elongated in time, which indicates that the combustion of the coal pellet slows down. In other words, the sodium contained in coal has catalytic effects to accelerate the combustion. In contrast to the general trend that the removal of sodium results in a slower combustion, the temperature increase and diameter decrease of the NH_4Ac treated sample are found to be enhanced at the devolatilization and initial period of char burnout stages, as shown in the zoomed in region of Fig. 5. This is because chemical extraction using NH_4Ac acid can influence the microcrystalline structure of the coal, leading to more micro-pores on coal surface [39]. Oxygen molecules are more easily absorbed by the coal, and therefore the heterogeneous combustion becomes enhanced.

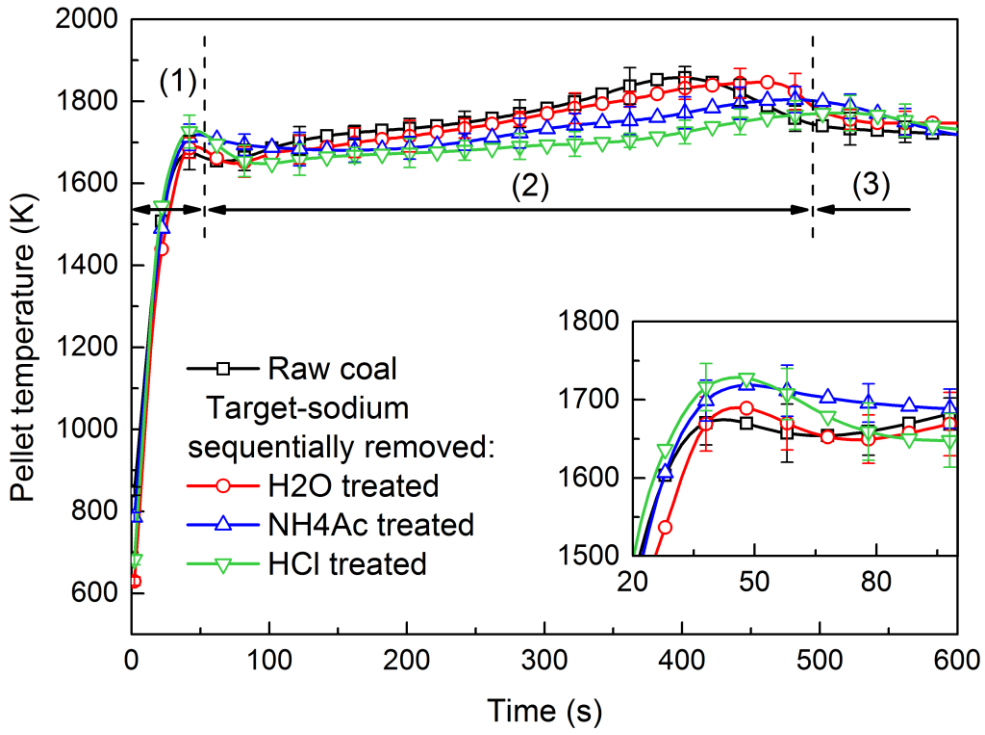

(a) Surface temperature of coal pellets

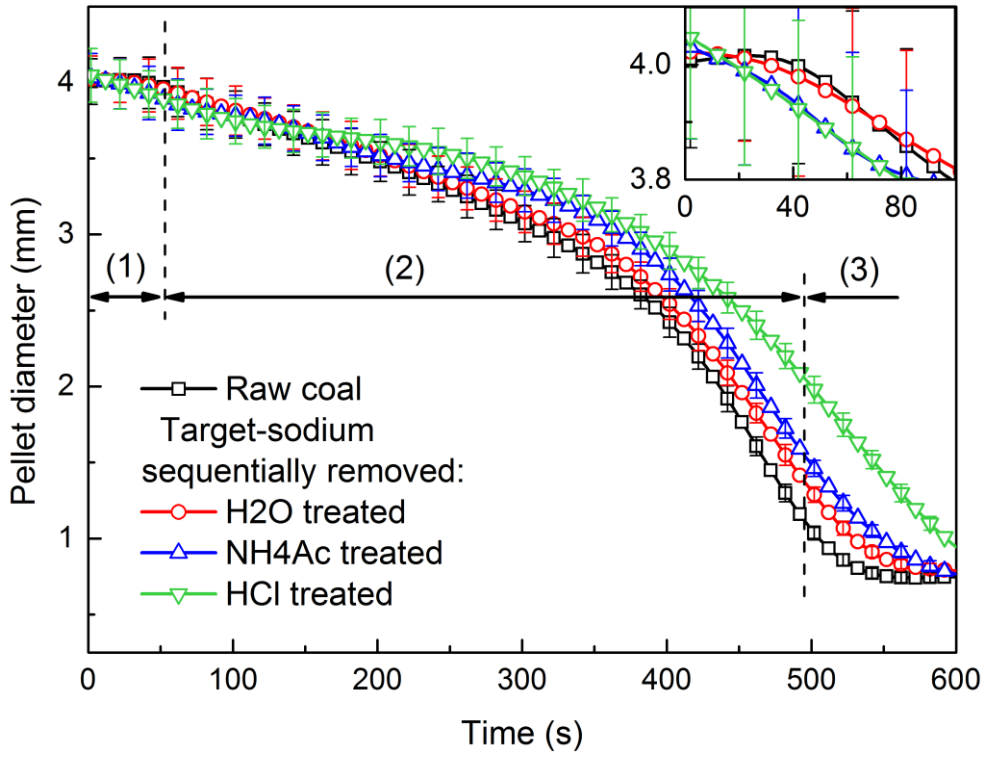

(b) Diameter of coal pellets

Fig. 5. Temporal profiles of surface temperature and diameter of coal pellets for raw and target-sodium sequentially removed Zhundong coal. Three combustion stages for the raw coal pellet are illustrated: (1) devolatilization, (2) char burnout, (3) ash cooking. The first 100 s has been

zoomed in and shown on the upper right.

Figure 6 illustrates the catalytic effects of different forms of enriched H_2O-soluble sodium on Zhundong coal pellet combustion. With target-sodium enrichment, the burning periods characterized by pellet temperature and diameter become shorter, indicating all the three sodium additives have catalytic effects to accelerate the coal pellet combustion (burnout time decreased by more than 5.7%). In general, sodium can weaken the bond of (C-O) and therefore enhance the heterogeneous reaction rate of coal [26]. With the same dosing ratio by weight, the catalytic effects on coal combustion is found in the order of NaOH > Na_2SO_4 > NaCl. NaOH has the strongest catalytic effects (burnout time decreased by 36.8%) due to the following two reasons. First, NaOH can be absorbed by the carbon structures and causes electron transference to increase the reactive of char [40]. Second, NaOH can have thermal decomposition under high temperature and form a redox pair of Na_2O and Na_xO_y which leads to an oxidation-reduction cycle promoting the electron transference between the char and oxygen [41]. Moreover, the enriched mass of sodium element is the highest for the same amount of sodium additives in the NaOH-enriched case (see Table 5). NaCl has the lowest catalytic effects because the combination of Cl with Na can prevents Na from becoming an active catalyst [42].

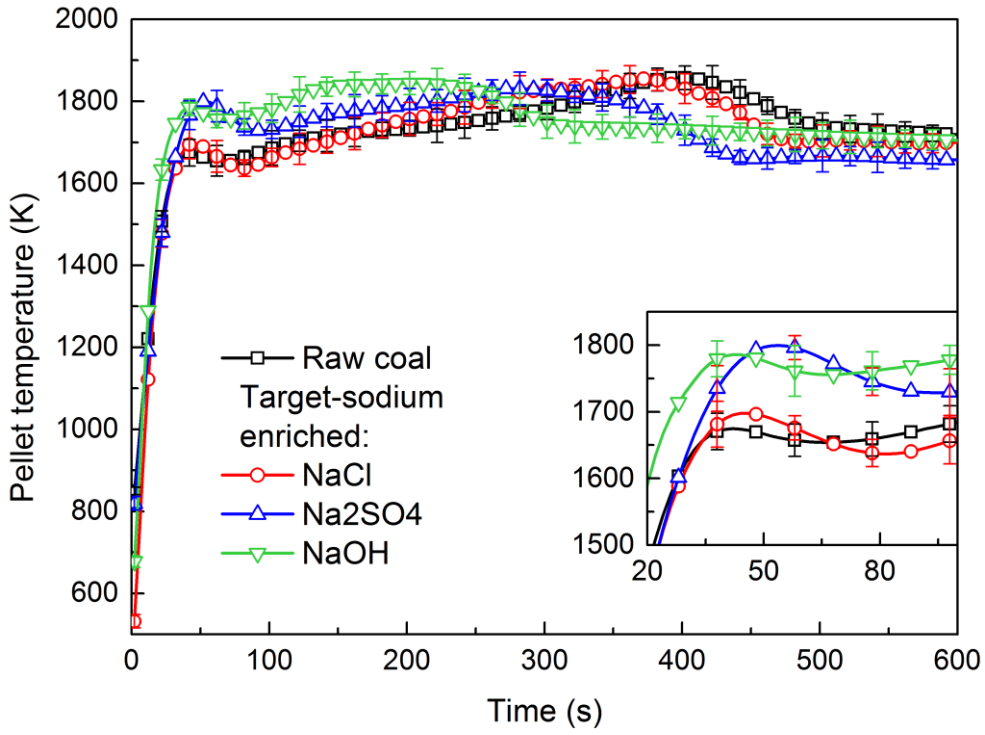

(a) Surface temperature of coal pellets

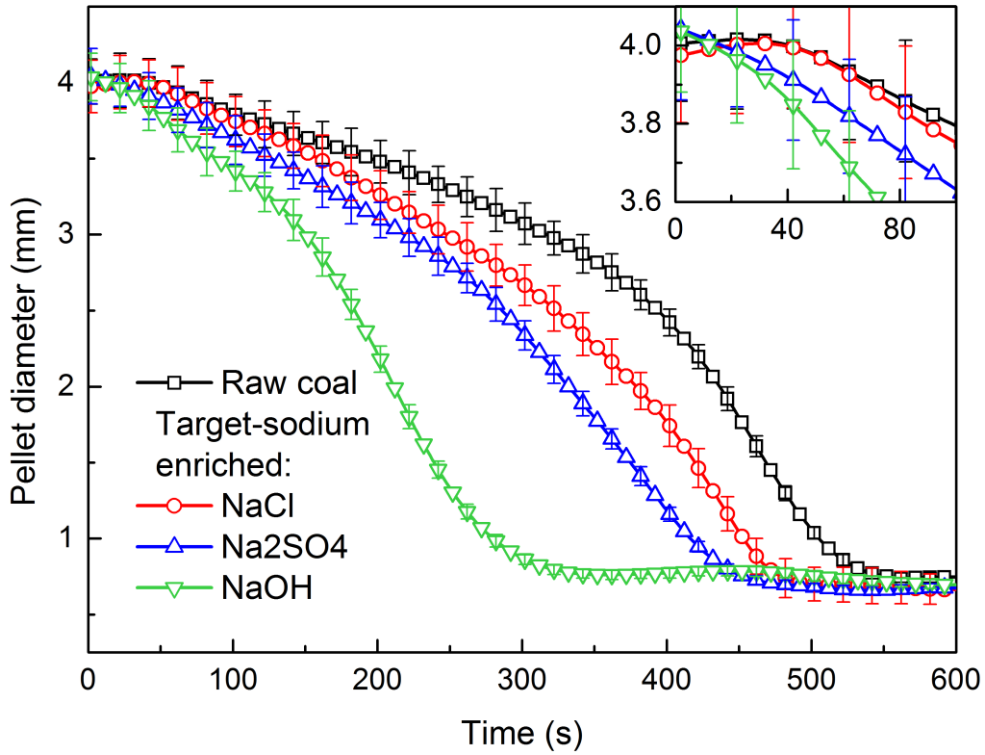

(b) Diameter of coal pellets

Fig. 6. Temporal profiles of surface temperature and diameter of coal pellets for raw and target-sodium enriched Zhundong coal. The first 100 s has been zoomed in and shown on the upper right.

4. Conclusions

The release characteristics and catalytic effects of different chemical forms of sodium during the combustion of Zhundong coal pellet have been investigated using a combination of two in-situ measurement techniques, i.e., multi-point LIBS and two-color pyrometry. First, the combustion of raw and target-sodium sequentially removed Zhundong coal pellets are studied. H_2O-soluble sodium, which contributes to 76% of the total sodium released, is found to be the major chemical form of sodium released in every stage of coal pellet combustion. It also shows the highest volatility, as 90.1% of the H_2O-soluble sodium contained in the coal is released into the gas phase. The insoluble sodium is found to be stable and only 2.3% of it is released. Different chemical forms of sodium, i.e., H_2O-soluble, NH_4Ac-soluble and HCl-soluble sodium, are found to introduce acceleration effects on the coal combustion.

Three common forms of H_2O-soluble sodium in coal, i.e., NaCl, NaOH and Na_2SO_4, are then enriched into the raw Zhundong coal to study their release characteristics and catalytic effects. The release characteristics of the enriched H_2O-soluble sodium are different from the H_2O-soluble sodium originally contained in the raw coal, which reveals the complexity of sodium behavior during coal combustion. For the same amount of sodium additives, the catalytic effects on coal combustion are found in the order of NaOH > Na_2SO_4 > NaCl. For the coal pellet enriched with NaOH, its burnout time is decreased by 36.8%.

Our future work will extend the study to the effects of other forms of H_2O-soluble, NH4Ac-soluble, HCl-soluble and insoluble sodium on the coal combustion process using the present target-sodium treatment approach.

Acknowledgements

This work was supported by the National Natural Science Foundation of China (51706200, 51776185, 51422605, 51621005), Project funded by China Postdoctoral Science Foundation (2018M632460), the Fundamental Research Funds for the Central Universities (2018FZA4012). Y.L. is funded by the Open Topic Exploration Program of the ZJU CEU laboratory.

References

(1) Khatami, R.; Levendis, Y. A. An overview of coal rank influence on ignition and combustion phenomena at the particle level. *Combust. Flame* **2016,** *164*, 22-34.
(2) Liu, Y. Z.; Wang, Z. H.; Lv, Y.; Wan, K. D.; He, Y.; Xia, J.; Cen, K. F. Inhibition of sodium release from Zhundong coal via the addition of mineral additives: A combination of online multi-point LIBS and offline experimental measurements. *Fuel* **2018,** *212*, 498-505.
(3) Wan, K. D.; Xia, J.; Wang, Z. H.; Pourkashanian, M.; Cen, K. F. Large-eddy Simulation of Pilot-assisted Pulverized-coal Combustion in a Weakly Turbulent Jet. *Flow Turbul. Combust.* **2017,** *99* (2), 531-550.
(4) Wan, K. D.; Xia, J.; Wang, Z. H.; Wrobel, L. C.; Cen, K. F. Online-CPD-coupled large-eddy simulation of pulverized-coal pyrolysis in a hot turbulent nitrogen jet. *Combust. Sci. Technol.* **2017,** *189* (1), 103-131.
(5) Li, R.; Kai, X.; Yang, T.; Sun, Y.; He, Y.; Shen, S. Release and transformation of alkali metals during co-combustion of coal and sulfur-rich wheat straw. *Energy Convers. Manage.* **2014,** *83*, 197-202.
(6) Wan, K. D.; Xia, J.; Vervisch, L.; Liu, Y. Z.; Wang, Z. H.; Cen, K. F. Modelling alkali metal emissions in large-eddy simulation of a preheated pulverised-coal turbulent jet flame using tabulated chemistry. *Combust. Theory Model.* **2017**, 1-34.
(7) Jiang, S.; Shen, L.; Niu, X.; Ge, H.; Gu, H. Chemical Looping Co-combustion of Sewage Sludge and Zhundong Coal with Natural Hematite as the Oxygen Carrier. *Energy Fuels* **2016,** *30* (3), 1720-1729.
(8) Song, G.; Song, W.; Qi, X.; Lu, Q. Transformation Characteristics of Sodium of Zhundong Coal Combustion/Gasification in Circulating Fluidized Bed. *Energy Fuels* **2016,** *30* (4), 3473-3478.
(9) Wu, X.; Zhang, X.; Yan, K.; Chen, N.; Zhang, J.; Xu, X.; Dai, B.; Zhang, J.; Zhang, L. Ash deposition and slagging behavior of Chinese Xinjiang high-alkali coal in 3 MWth pilot-scale combustion test. *Fuel* **2016,** *181*, 1191-1202.
(10) Song, G.; Qi, X.; Song, W.; Lu, Q. Slagging Characteristics of Zhundong Coal during Circulating Fluidized Bed Gasification. *Energy Fuels* **2016,** *30* (5), 3967-3974.
(11) Yu, H.; Niu, S.; Lu, C.; Li, J.; Yang, Y. Preparation and esterification performance of sulfonated coal-based heterogeneous acid catalyst for methyl oleate production. *Energy Convers. Manage.* **2016,**

126, 488-496.
(12) Li, G.; Wang, C. a.; Yan, Y.; Jin, X.; Liu, Y.; Che, D. Release and transformation of sodium during combustion of Zhundong coals. *J. Energy Inst.* **2016,** *89* (1), 48-56.
(13) Quann, R. J.; Neville, M.; Janghorbani, M.; Mims, C. A.; Sarofim, A. F. Mineral matter and trace-element vaporization in a laboratory-pulverized coal combustion system. *Environ. Sci. Technol.* **1982,** *16* (11), 776-781.
(14) Greger, F.; Hartinger, K. T.; Monkhouse, P. B.; Wolfrum, J.; Baumann, H.; Bonn, B. In situ alkali concentration measurements in a pressuried, fluidized-bed coal combustor by excimer laser induced fragmentation fluorescence. *Symposium on Combust* **1996,** *26* (2), 3301-3307.
(15) Schlosser, E.; Fernholz, T.; Teichert, H.; Ebert, V. In situ detection of potassium atoms in high-temperature coal-combustion systems using near-infrared-diode lasers. *Spectroc. Acta Pt. A-Molec.* **2002,** *58* (11), 2347-2359.
(16) van Eyk, P. J.; Ashman, P. J.; Alwahabi, Z. T.; Nathan, G. J. Quantitative measurement of atomic sodium in the plume of a single burning coal particle. *Combust. Flame* **2008,** *155* (3), 529-537.
(17) He, Y.; Zhu, J.; Li, B.; Wang, Z.; Li, Z.; Aldén, M.; Cen, K. In-situ Measurement of Sodium and Potassium Release during Oxy-Fuel Combustion of Lignite using Laser-Induced Breakdown Spectroscopy: Effects of O2 and CO2 Concentration. *Energy Fuels* **2013,** *27* (2), 1123-1130.
(18) Wang, Z. H.; Liu, Y. Z.; Whiddon, R.; Wan, K. D.; He, Y.; Xia, J.; Cen, K. F. Measurement of atomic sodium release during pyrolysis and combustion of sodium-enriched Zhundong coal pellet. *Combust. Flame* **2017,** *176*, 429-438.
(19) Liu, Y. Z.; He, Y.; Wang, Z. H.; Wan, K. D.; Xia, J.; Liu, J. Z.; Cen, K. F. Multi-point LIBS measurement and kinetics modeling of sodium release from a burning Zhundong coal particle. *Combust. Flame* **2018,** *189*, 77-86.
(20) Benson, S. A.; Holm, P. L. Comparison of inorganic constituents in three low-rank coals. *Ind. Eng. Chem. Prod. Res. Dev.* **1985,** *24* (1).
(21) Zhang, J.; Han, C.-L.; Yan, Z.; Liu, K.; Xu, Y.; Sheng, C.-D.; Pan, W.-P. The Varying Characterization of Alkali Metals (Na, K) from Coal during the Initial Stage of Coal Combustion. *Energy Fuels* **2001,** *15* (4), 786-793.
(22) Liu, Y.; Cheng, L.; Zhao, Y.; Ji, J.; Wang, Q.; Luo, Z.; Bai, Y. Transformation behavior of alkali metals in high-alkali coals. *Fuel Process. Technol.* **2018,** *169*, 288-294.
(23) Li, R.; Chen, Q.; Zhang, H. Detailed Investigation on Sodium (Na) Species Release and Transformation Mechanism during Pyrolysis and Char Gasification of High-Na Zhundong Coal. *Energy Fuels* **2017,** *31* (6), 5902-5912.
(24) Van Eyk, P. J.; Ashman, P. J.; Alwahabi, Z. T.; Nathan, G. J. The release of water-bound and organic sodium from Loy Yang coal during the combustion of single particles in a flat flame. *Combust. Flame* **2011,** *158* (6), 1181-1192.
(25) Hu, B.; Huang, Q.; Buekens, A.; Chi, Y.; Yan, J. Co-gasification of municipal solid waste with high alkali coal char in a three-stage gasifier. *Energy Convers. Manage.* **2017,** *153*, 473-481.
(26) Kuang, J.-p.; Zhou, J.-h.; Zhou, Z.-j.; Liu, J.-z.; Cen, K.-f. Catalytic mechanism of sodium compounds in black liquor during gasification of coal black liquor slurry. *Energy Conv. Manag.* **2008,** *49* (2), 247-256.
(27) Nzihou, A.; Stanmore, B.; Sharrock, P. A review of catalysts for the gasification of biomass char, with some reference to coal. *Energy* **2013,** *58*, 305-317.
(28) Lahijani, P.; Zainal, Z. A.; Mohamed, A. R.; Mohammadi, M. CO2 gasification reactivity of biomass char: Catalytic influence of alkali, alkaline earth and transition metal salts. *Bioresour.*

Technol. **2013,** *144*, 288-295.
(29) Tang, J.; Wang, J. Catalytic steam gasification of coal char with alkali carbonates: A study on their synergic effects with calcium hydroxide. *Fuel Process. Technol.* **2016,** *142*, 34-41.
(30) Kirtania, K.; Axelsson, J.; Matsakas, L.; Christakopoulos, P.; Umeki, K.; Furusjö, E. Kinetic study of catalytic gasification of wood char impregnated with different alkali salts. *Energy* **2017,** *118*, 1055-1065.
(31) Liu, Y.; Wang, Y.; Guo, F.; Li, X.; Li, T.; Guo, C.; Chang, J. Characterization of the gas releasing behaviors of catalytic pyrolysis of rice husk using potassium over a micro-fluidized bed reactor. *Energy Conv. Manag.* **2017,** *136*, 395-403.
(32) He, Y.; Qiu, K. Z.; Whiddon, R.; Wang, Z. H.; Zhu, Y. Q.; Liu, Y. Z.; Li, Z. S.; Cen, K. F. Release characteristic of different classes of sodium during combustion of Zhun-Dong coal investigated by laser-induced breakdown spectroscopy. *Sci. Bull.* **2015,** *60* (22), 1927-1934.
(33) Smith, G. P.; Golden, D. M.; Frenklach, M.; Moriarty, N. W.; Eiteneer, B.; Goldenberg, M.; Bowman, C. T.; Hanson, R. K.; Song, S.; Gardiner Jr, W. C. GRI 3.0 Mechanism. *Gas Research Institute, Des Plaines, IL, accessed Aug* **1999,** *21*, 2017.
(34) He, Y.; Zhu, J. J.; Li, B.; Wang, Z. H.; Li, Z. S.; Aldén, M.; Cen, K. F. In-situ measurement of sodium and potassium release during oxy-fuel combustion of lignite using laser-induced breakdown spectroscopy: effects of O2 and CO2 concentration. *Energy Fuels* **2013,** *27* (2), 1123-1130.
(35) Huang, Y.; Yan, Y.; Riley, G. Vision-based measurement of temperature distribution in a 500-kW model furnace using the two-colour method. *Measurement* **2000,** *28* (3), 175-183.
(36) DeWitt, D. P.; Nutter, G. D. *Theory and practice of radiation thermometry*. Wiley Online Library: 1988.
(37) van Eyk, P. J.; Ashman, P. J.; Alwahabi, Z. T.; Nathan, G. J. Simultaneous measurements of the release of atomic sodium, particle diameter and particle temperature for a single burning coal particle. *Proc. Combust. Inst.* **2009,** *32* (2), 2099-2106.
(38) Van Eyk, P. J.; Ashman, P. J.; Nathan, G. J. Mechanism and kinetics of sodium release from brown coal char particles during combustion. *Combust. Flame* **2011,** *158* (12), 2512-2523.
(39) Zhang, L.; Li, Z.; Yang, Y.; Zhou, Y.; Kong, B.; Li, J.; Si, L. Effect of acid treatment on the characteristics and structures of high-sulfur bituminous coal. *Fuel* **2016,** *184*, 418-429.
(40) Kelemen, S. R.; Mims, C. A. The interaction of KOH with the basal surface of graphite. *Surf. Sci.* **1983,** *133* (1), 71-88.
(41) J. Ulán-Gómez, M.; Linares-Solano, A.; Radovic, L. R.; Salinas-Martínez de Lecea, C., No reduction by activated carbons. some mechanistic aspects of uncatalyzed and catalyzed reaction. In *Coal Sci Technol*, Pajares, J. A.; Tascón, J. M. D., Eds. Elsevier: 1995; Vol. 24, pp 1799-1802.
(42) Quyn, D. M.; Wu, H.; Hayashi, J.-i.; Li, C.-Z. Volatilisation and catalytic effects of alkali and alkaline earth metallic species during the pyrolysis and gasification of Victorian brown coal. Part IV. Catalytic effects of NaCl and ion-exchangeable Na in coal on char reactivity☆. *Fuel* **2003,** *82* (5), 587-593.

Figure captions

Fig. 1. Multi-point LIBS experimental setup.

Fig. 2. Temporal sodium release profiles of raw and target-sodium sequentially removed Zhundong coal measured by the multi-point LIBS. Three combustion stages for the raw coal pellet are illustrated: (1) devolatilization, (2) char burnout, and (3) ash cooking. The NH_4Ac and HCl treated cases have been zoomed in and shown on the bottom.

Fig. 3. Contribution of different chemical forms of sodium to the mass of sodium released in the three stages of coal pellet combustion.

Fig. 4. (a) Temporal sodium release profiles of raw and target-sodium enriched Zhundong coal measured by single-point LIBS. (b) Time-normalized temporal release profiles. The time has been normalized by the characteristic time at the termination of char burnout in each case. Profiles of the raw coal and originally contained H_2O-soluble sodium are also shown.

Fig. 5. Temporal profiles of surface temperature and diameter of coal pellets for raw and target-sodium sequentially removed Zhundong coal. Three combustion stages for the raw coal pellet are illustrated: (1) devolatilization, (2) char burnout, (3) ash cooking. The first 100 s has been zoomed in and shown on the upper right.

Fig. 6. Temporal profiles of surface temperature and diameter of coal pellets for raw and target-sodium enriched Zhundong coal. The first 100 s has been zoomed in and shown on the upper right.

Color figures can be used for the online PDF version and the gray style for hardcopy reproduction.